Vibrational Modes and IR Analysis of Neutral Photopolymerized C60 Dimers

doi: 10.1103/PhysRevB.57.223

Vibrational modes and IR analysis of neutral photopolymerized C_{60} dimers

Keivan Esfarjani
Institute for Materials Research, Tohoku University, Sendai 980-77, Japan

Yuichi Hashi
Research and Development Center, Hitachi Tohoku Software Ltd., Sendai 980, Japan

Jun Onoe and Kazuo Takeuchi
The Institute of Physical and Chemical Research (RIKEN), 2-1 Hirosawa, Wako, Saitama 351-01, Japan

Yoshiyuki Kawazoe
Institute for Materials Research, Tohoku University, Sendai 980-77, Japan

(Received 17 June 1997)

Motivated by recent experiments on C_{60} dimers, we have performed total-energy minimizations for several isomers of the C_{60} dimer in the neutral configuration in order to find the ground-state structure. The phonon spectra and electronic energy levels have also been calculated within the generalized tight-binding approximation. From these calculations, one can also deduce the IR absorption spectrum. By comparing our results with the available IR experimental data, we can draw conclusions regarding the structure of the C_{60} dimer used in the experiments. [S0163-1829(98)00301-4]

I. INTRODUCTION

Recently, there has been much interest in studying the ground-state configuration of the C_{60} dimer.[1–7] Indeed the latter is important in determining the configuration of polymerized solid fullerenes that have one-, two-, and three-dimensional structures. The polymerized phase has been reported to appear at high temperature and high pressure.[8] After laser irradiation of pristine fullerene films deposited on silicon surface, with relatively high intensity, fullerene clusters that are bound with forces other than the usual Van der Waals type can also be produced. These clusters maybe composed of two, three, four, ... up to seven C_{60} molecules.[9] There is therefore high interest in investigating the nature of this bonding. It is possible to probe the vibrational properties of these clusters by infrared (IR) (Ref. 10) and Raman techniques among others, to obtain structural information on these systems. These experimental results can be compared to tight-binding calculations of the spectrum from which one can also distinguish the IR and Raman contributions. It is the purpose of this paper to perform such a study in order to deduce the structure of the dimer clusters. Here, we report on a quantitative confirmation that the structure of the dimer observed in photopolymerization experiments is the $[2+2]$ cycloaddition (see Fig. 1), by directly comparing the calculated and experimental IR absorption spectra. This is a powerful method for identification of the structure of isomers of a cluster or a solid. Previously mentioned publications report either theoretical calculations or experimental results on the IR spectrum.

II. THEORY

A. Tight-binding (TB) model and geometry optimization

The number of atoms being large (120 atoms), a local-density approximation (LDA) calculation involving full geometry optimization, vibrational frequency, and IR spectrum calculation is indeed out of reach of many powerful supercomputers. This is why in this paper we have adopted the TB method for calculating the electronic structure as well as the total energy and the vibrational spectrum of several of the candidate isomers. We have used the formulation proposed by Xu *et al.*[11] in which the total energy is written as a sum of single-particle energy eigenvalues and a short-range repulsive term of the form

$$E_{\rm rep}=\sum_i f\left(\sum_j \phi(r_{ij})\right), \tag{1}$$

$$\phi(r)=\begin{cases}\phi_0\left(\dfrac{d_0}{r}\right)^m \exp\left\{m\left[-\left(\dfrac{r}{d_c}\right)^{m_c}+\left(\dfrac{d_0}{d_c}\right)^{m_c}\right]\right\}, & r<d_1\\ c_0+c_1(r-d_1)+c_2(r-d_1)^2+c_3(r-d_1)^3, & r\geqslant d_1,\end{cases} \tag{2}$$

where

$$f(x)=a_0+a_1x+a_2x^2+a_3x^3+a_4x^4. \tag{3}$$

The Slater-Koster parameters are also written as follows:

$$V(r_{ij})=V(r_0)S(r_{ij}),$$

$$S(r)=\begin{cases}\left(\dfrac{r_0}{r}\right)^n \exp\left\{n\left[-\left(\dfrac{r}{r_c}\right)^{n_c}+\left(\dfrac{r_0}{r_c}\right)^{n_c}\right]\right\}, & r<r_1\\ d_0+d_1(r-r_1)+d_2(r-r_1)^2+d_3(r-r_1)^3, & r\geqslant r_1,\end{cases} \tag{4}$$

TABLE I. Comparison between the experimental and calculated IR intensities for C_{60} by TB, MNDO and two different LDA calculations. The frequencies are in cm^{-1}.

TB (present)		MNDO (Ref. 15)		LDA (Ref. 16)		LDA (Ref. 13)		Experiment (Ref. 10)	
ω	Intensity	ω	Intensity	ω	Intensity	ω	Intensity	ω	Intensity
486	1.00	504	1.00	527	1.00	516	1.00	527	1.00
600	0.08	626	0.35	586	0.63	557	0.65	576	0.30
1199	0.18	1179	1.87	1218	0.36	1202	0.59	1183	0.22
1571	1.74	1419	4.35	1462	0.57	1589	0.41	1429	0.24

where $r_0, r_1, r_c, n, n_c, m, m_c, d_0$, and d_c are appropriate tight-binding parameters. In general, the LDA cohesive energy curves of graphite and diamond are reproduced very accurately with this orthogonal scheme, which has also predicted well the atomic coordinates and bond lengths of C_{60}.

The structures are relaxed to their minimum energy by using Newton's method: taking a finite difference of the forces, which are computed analytically, one can compute the Hessian matrix, whose eigenvalues and eigenvectors allow us to displace the atoms according to the following equation in which F is the $3N$-dimensional force vector:

$$\delta x = -(\nabla F)^{-1} \cdot F.$$

In the last iteration where the system is fully relaxed, this second derivative matrix of the total-energy [in other words: $(-\nabla F)^{-1}$] is just the dynamical matrix whose eigenvalues are the square of the vibrational frequencies of the system.

B. IR calculation method

To calculate the IR intensities of each of the vibrational modes, we can either use the finite difference method,[12] or the linear-response theory[13] to compute the effective charge tensor. In the finite difference method, one calculates the change in the dipole moment after a small distorsion along the vibrational mode is applied to the system. The IR intensity is given by the square of this change:

$$I_\lambda \propto |D(\lambda) - D_0|^2, \tag{5}$$

where D_0 is the permanent dipole moment and $D(\lambda)$ is the dipole moment of the distorted cluster along the vibrational mode λ. In the linear-response formalism, one computes the same expression by calculating the difference analytically; in other words, by computing the first-order term in the Taylor expansion of the dipole moment:

$$I_\lambda \propto \sum_{\alpha=1,3} \left| \sum_{\substack{i=1,N \\ \beta=1,3}} \nabla_{i\beta} D^\alpha e_i^\beta(\lambda) \right|^2, \tag{6}$$

where $e_i^\beta(\lambda)$ is the β component of the polarization vector of mode λ on atom i. The effective charge tensor, $Z = \nabla D$ is calculated from linear response (or perturbation theory):

$$\nabla_{i\beta} D^\alpha = Z_i^{\alpha\beta} = \int \nabla_{i\beta} \rho(r) r^\alpha d^3 r - Z_i \delta_{\alpha\beta}. \tag{7}$$

Here Z_i is the nucleus charge, and $\rho(r)$ is the total electronic charge density:

$$\rho(r) = 2 \sum_{\mu}^{\text{occ}} |\psi_\mu(r)|^2. \tag{8}$$

Under the ''infinitesimal'' displacement along the phonon mode, one can calculate the change in the electronic eigenstates by using first-order perturbation theory:

$$\psi'_\mu(r) = \psi_\mu(r) + \sum_{\nu \neq \mu} \psi_\nu(r) \frac{\langle \psi_\nu | V | \psi_\mu \rangle}{E_\mu - E_\nu}. \tag{9}$$

The perturbation V is just the difference between the perturbed and the unperturbed Hamiltonians: $V = H(R+e) - H(R) = e \cdot \nabla H$. In the generalized tight-binding molecular dynamics (TBMD) formalism, the matrix elements of the Hamiltonian are known analytically, and one can therefore easily calculate the matrix elements of the per-

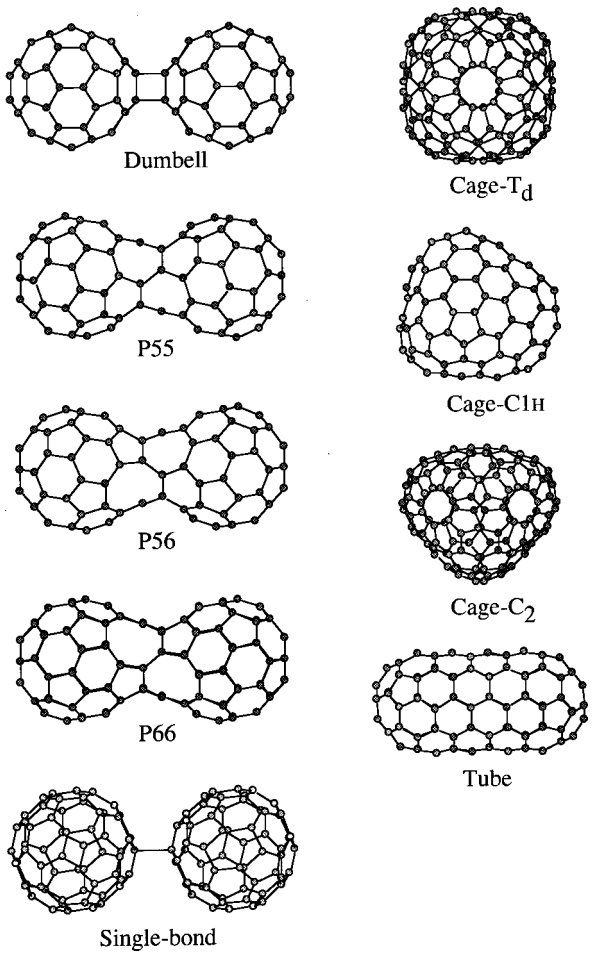

FIG. 1. Geometry of the nine considered isomers.

TABLE II. Electronic and geometrical properties of the nine candidates for photopolymerized C_{60}.

Isomer	Symmetry	Binding energy (eV)	Gap (eV)	Intersphere distance (Å)
Dumbell	D_{2h}	0.413	1.7981	9.0847
Single-B		−0.049	1.6336	9.2529
$P55$	D_{3d}	−2.783	1.8797	8.5194
$P56$	C_{3v}	−0.177	1.6548	8.5735
$P66$	D_{3d}	2.187	1.4199	8.6188
Cage-T_d	T_d	−17.066	1.6617	
Cage-C_{1h}	C_{1h}	−16.616	1.6462	
Cage-C_2	C_2	−16.637	1.6443	
Tube	D_{5d}	−14.533	0.8040	

turbation V by using the Hellman-Feynmann theorem. The final result for the effective charge matrix can be written as follows:

$$Z_i^{\alpha\beta}=\sum_{\mu}^{\text{occ}}\sum_{\nu}^{\text{unocc}}\frac{4}{E_\mu-E_\nu}\langle\nu|r^\alpha|\mu\rangle\langle\mu|\nabla_i^\beta H|\nu\rangle-Z_i\delta_{\alpha\beta}, \tag{10}$$

where the first sum is over *occupied*, and the second sum over *unoccupied* orbitals. This general expression can be used within any one-particle formalism (Hartree-Fock, LDA, TB, etc.). The wave functions $|\psi_\nu\rangle$ are the eigenstates of the unperturbed one-particle Hamiltonian with eigenvalues E_ν.

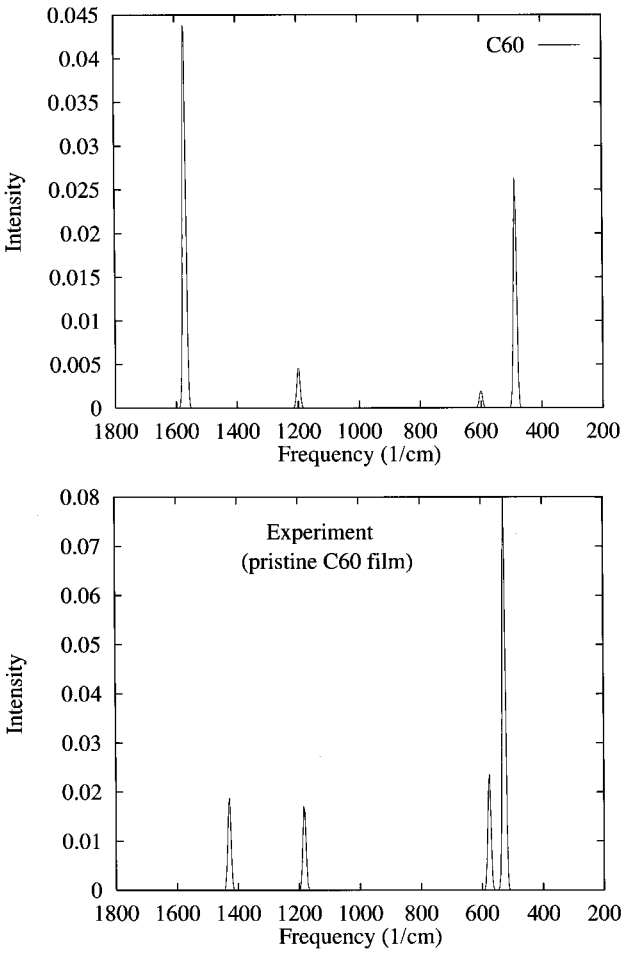

FIG. 2. Calculated and experimental IR intensities of C_{60}.

But in each formalism the calculation of the matrix elements of $\vec{r}$ or $\vec{\nabla}H$ are different. In our present TB case, the force matrix is calculated analytically, and its matrix elements in the basis of the eigenstates is readily computed. For the matrix elements of $\vec{r}$, however, the TB basis functions being orthonormal, one can use the following approximation:

$$\langle\nu|r^\alpha|\mu\rangle=\sum_{il}\sum_{jk}c_{il}^{\nu *}c_{jk}^{\mu}\delta_{ij}(\delta_{lk}R_i^\alpha+S_{lk}^\alpha), \tag{11}$$

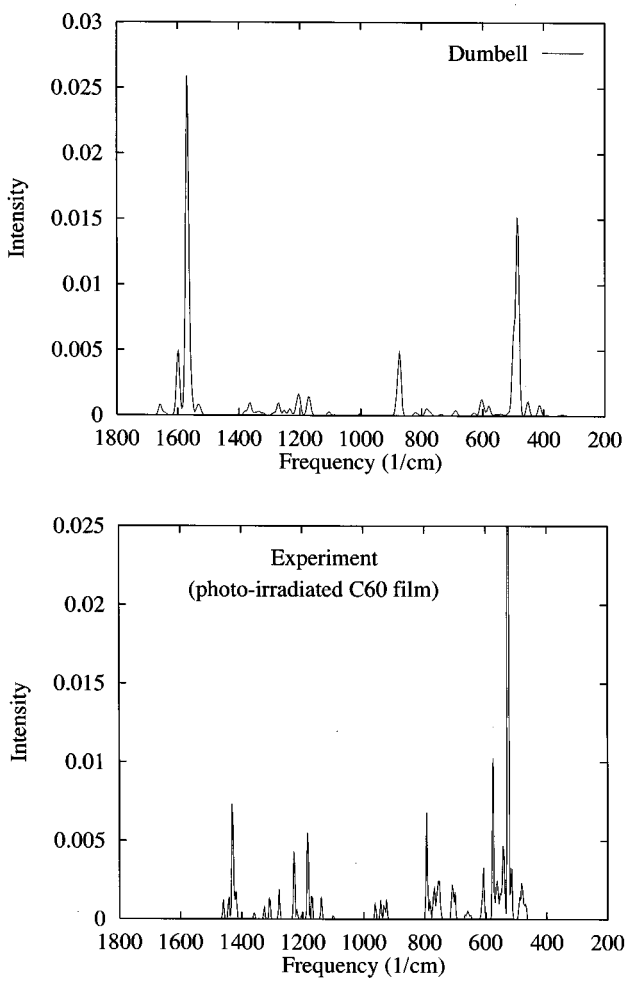

FIG. 3. Calculated IR intensities of the dumbell structure and the result of photopolymerization experiments.

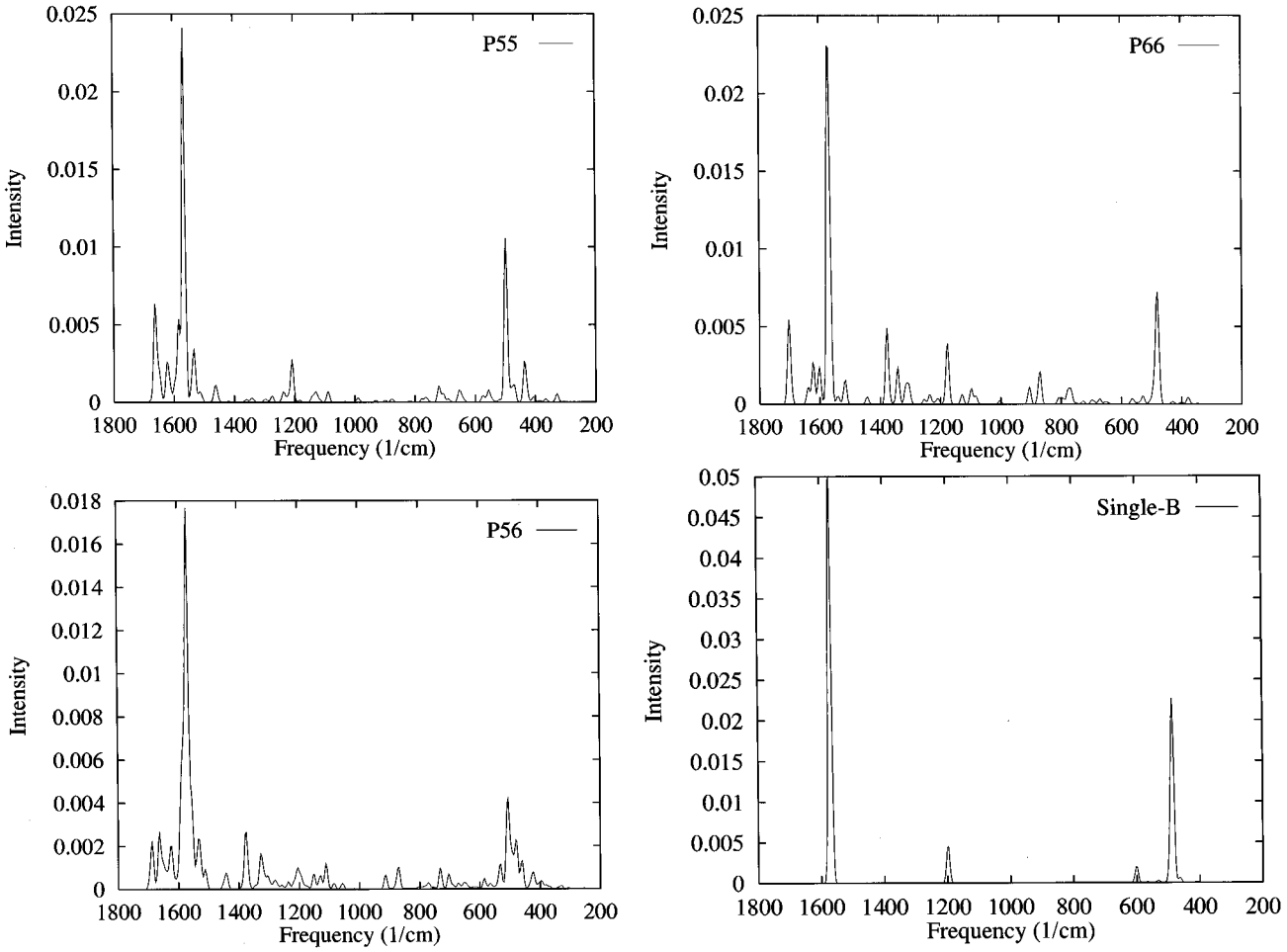

FIG. 4. Calculated IR intensities of the peanut shape and the single-bond structures.

where $S_{lk}^{\alpha}=\int \psi_{2s}(r)r^{\alpha}\psi_{2p_{\alpha}}(r)dr=S$ for $l=2s$ and $k=2p_{\alpha}$ and zero otherwise; the indices l,k refer to the orbitals and i,j refer to the atoms whose coordinates are represented by R. Finally, c_{jk}^{μ} are the coefficients of the expansion of the eigenfunction $|\mu\rangle$ on the basis set $|jk\rangle$. In our calculations, S is a free parameter which can be adjusted. We enforce the sum rule on the effective charge tensor Z to fix the value of S by minimizing the left-hand side of Eq. (12), since in perturbation treatment, the sum rule is not satisfied anymore. The sum rule

$$\sum_i Z_i^{\alpha\beta}=0 \tag{12}$$

comes from the fact that the dipole moment should not change for a random but uniform displacement of the atoms [see Eq. (7)]. The parameter S is found by imposing the above sum rule on C_{60} and then using the optimized value for the calculation of all other systems, since it should be the same as long as the used basis functions are the same. Among the two mentioned methods, we have chosen the finite difference one because it relies on ground-state properties, and has a better chance to be accurate. The linear-response formulation, involving the unoccupied or excited states, would be less accurate since the latter are not well approximated even by *ab initio* LDA-based methods. Furthermore the sum should extend over all the excited states, which in the TB case is quite limited, and hence inaccurate.

For a comparison between LDA, tight-binding, and modified neglect of differential overlap (MNDO) methods, one could refer to (Ref. 14), or Table I in which one can notice the change in the IR intensities even from one LDA to another LDA calculation. The TB results are still better than MNDO,[15] which predicts that the fourth peak is more than four times more intense than the first one, and the third peak almost twice the first one. Besides, to get better agreement with experiment, the MNDO frequencies have been scaled by a factor of 0.87.[15] One can see a comparison between the TB and experiment for the spectrum of C_{60} in Fig. 2. The frequencies agree reasonably well, but as far as the intensities of C_{120} isomers are concerned, one should compare the change of the peak intensities relative to that of C_{60}, between theory and experiment.

III. RESULTS AND DISCUSSION

A. General features of the spectra

We considered five C_{60} dimers and four C_{120} cages. The five C_{60} dimers correspond to Figs. 1(a), 3(a), 3(b), and 3(c) reported by Strout *et al.*[1] and are labeled here dumbell ([2+2] cycloaddition), $P66$, $P56$, and $P55$ (P represents peanuts), respectively. Additionally, we have also considered

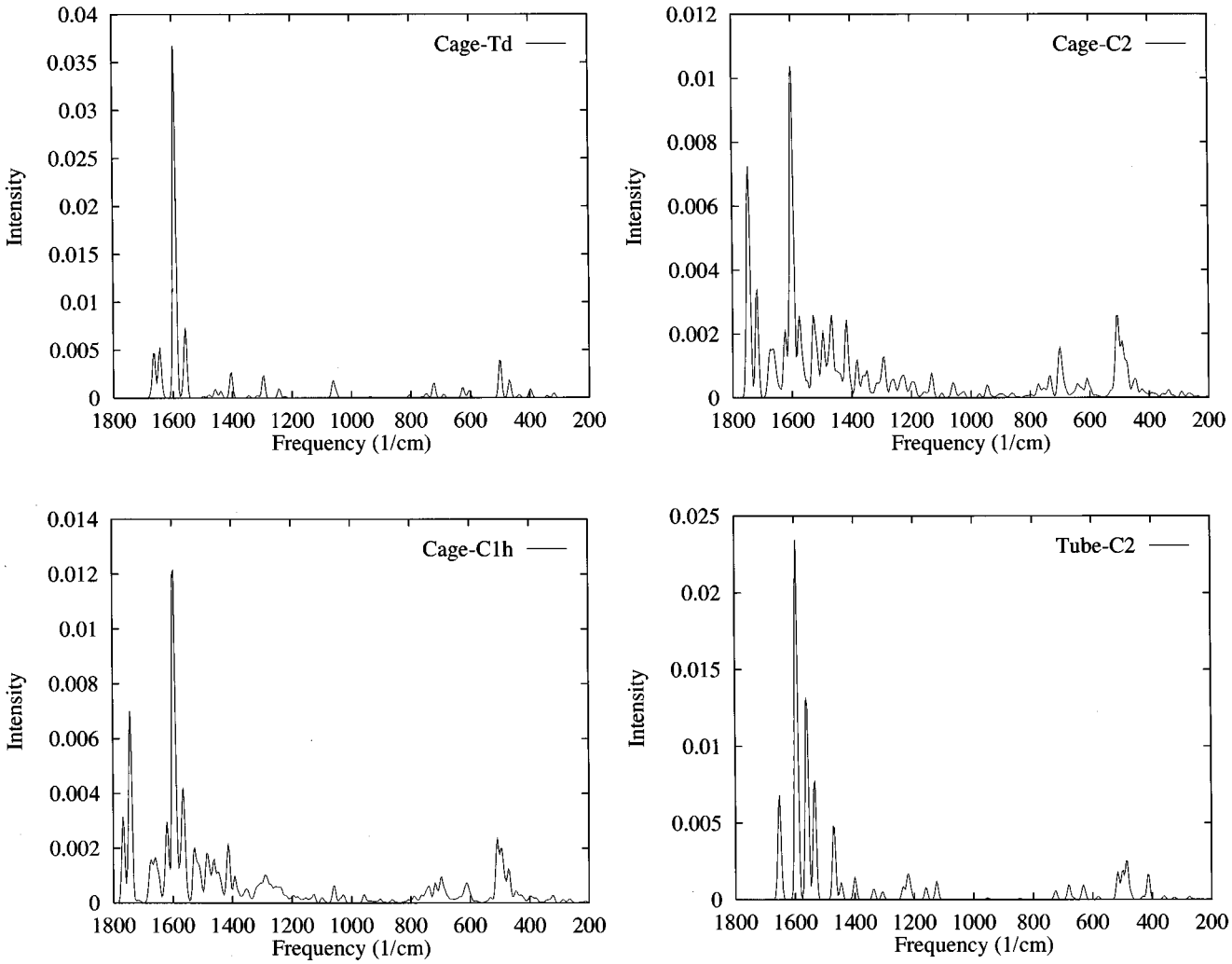

FIG. 5. Calculated IR intensities of the cage and tube structures.

the two C_{60} connected by a ''single bond.'' However, the four C_{120} cages are among the most energetically stable isomers of C_{120} fullerene.[17] Some of the electronic properties of these fullerenes are summarized in Table II, and their geometry can be viewed in Fig. 1.

The results of our TB calculations, which were obtained with $S=3.87$, are shown in Figs. 3, 4, and 5. This value of S was obtained by enforcing the sum rule [Eq. (12)] on C_{60} IR spectrum using the perturbation approach. However, as mentioned earlier, our calculations for C_{120} isomers are done by using the finite difference formula (5). For the sake of comparison with experiment, the peaks have been broadened with a Gaussian of width 5 cm^{-1}; all plotted intensities are in arbitrary units.

One can notice that for the single bond, the spectrum is almost the same as for C_{60} for which the four IR-active frequencies are: 487, 600, 1199, and 1571 cm^{-1}, respectively (see Table I). The latter results are in good agreement with experiment and other LDA-based *ab initio* methods. For the dumbell structure, a new peak appears at around 875 cm^{-1}, which can be associated with the strong 793 cm^{-1} peak of Onoe and Takeuchi[10] (see also Fig. 3). This is actually the superposition of two strong peaks at 871 and 880 cm^{-1}, respectively. The vibrations corresponding to these modes are displayed in Fig. 6. The 1199 cm^{-1} peak of C_{60} splits into several smaller ones at 1270, 1203, 1167, and 1173 cm^{-1}. Similarly, the 1571 cm^{-1} peak acquires three satellites at 1599, 1556, and 1657 cm^{-1}. These features as well as the 875 cm^{-1} peak compare well with the experimental results as can be seen from Fig. 3.

The IR spectra of the four cages displayed in Fig. 5 are different from the experiment in that we observe many relatively large peaks developed much above the 1571 cm^{-1} peak, and that lower frequency peaks have their intensity largely reduced. The cage structures can therefore be ruled out as candidates for the photopolymerized dimers observed in Ref. 10. Peanut-shape clusters have however, as can be seen from Fig. 4, features that are similar to the experiment, especially the $P66$ D_{3d} isomer. After a more careful comparison with the experimental data (Fig. 3), one can discard these structures as well since the many strong developed peaks at around 1200, 1400, and 1700 cm^{-1} do not appear in the experimental data and the 793 cm^{-1} peak of the experiment is absent in most of the considered structures (except for the dumbell and $P66$). Furthermore, generally because of their lower symmetry, these isomers have more broadly distributed peaks with lower intensities.

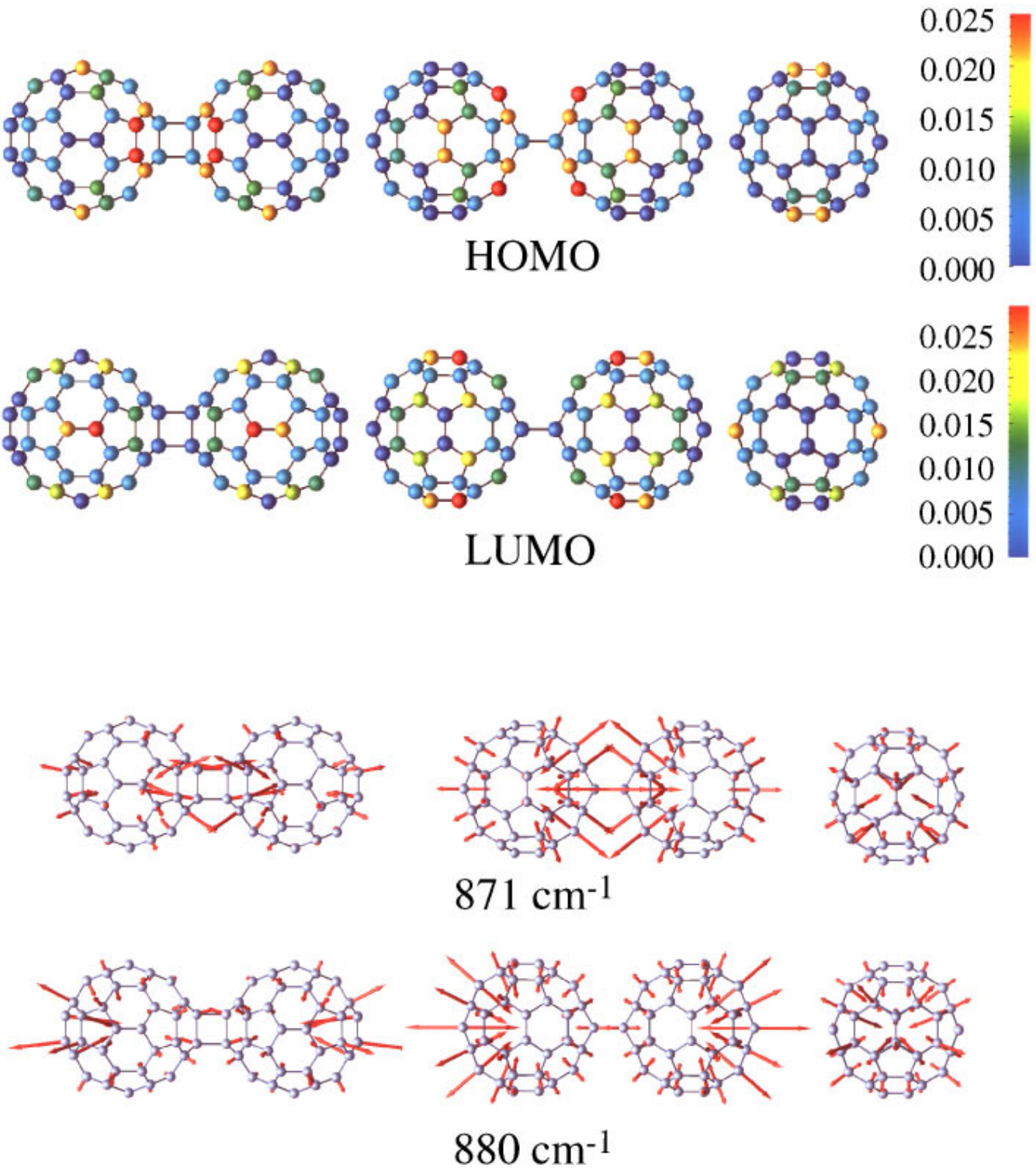

FIG. 6. (Color) (Top) Calculated HOMO and LUMO charge distributions of the dumbell structure. (Bottom) Vibrational modes of the 871 and 880 peaks. (From left to right: front, top, and side views).

B. Electronic structure and vibrational modes of the dumbell structure

In the case of the dumbell isomer, we have displayed in Fig. 6 the electronic charge of the highest occupied molecular orbitals (HOMO) and lowest unoccupied molecular orbitals (LUMO) levels of the cluster. One can notice that the HOMO charge is mostly localized *around* the connecting bonds, whereas the LUMO charge is more extended on the middle part of the C_{60} cage. These features are also shared by the peanut structures. In the same figure, we have shown the two characteristic vibrational modes at 875 cm^{-1}. Their symmetry, as well as the symmetry of the most strong peaks

of the spectrum is B_{3u}. One can again notice that these modes are also mostly localized *around* the connecting bonds.

The dumbell structure, thought to be the most likely candidate for the dimer[18,1] has been found by us and other authors to have a positive binding energy. All these calculations, are based on the tight-binding method, which is, pretty much like (but still not as good as) density-functional (DF) calculations, unable to take the Van der Waals (VdW) interactions correctly into account. Therefore, *the total-energy results* concerning this structure, as well as the single bond which was also found to have a positive binding energy, might not be as reliable as other structures, since VdW interactions play an important role in these isomers.

We find that the lowest vibrational frequencies of the dumbell are about 18, 22, and 30 cm^{-1}. They correspond to bending modes of the double bond connecting the two cages in-plane and out-of-plane. The high-frequency modes appearing at 1660 cm^{-1} also relate to this double bond, but this time, the stretching modes are localized *around* the bond. The proper stretching of the bond is at much lower frequencies around 800 cm^{-1}, as shown in Fig. 6.

Other low-frequency modes correspond, for example, to dilation of one cage, while the other one is compressed (226 cm^{-1}), or uneven flattening of the two cages (266 cm^{-1}).

IV. SUMMARY

For the calculation of the IR spectrum, because of the limitations in treating 120 atoms with DF-LDA methods, we have used the tight-binding approach, which for larger fullerenes is still tractable on large computers. This method is successful in predicting the ground-state geometry of carbon clusters as well as their vibrational frequencies, in some instances as accurately as *ab initio* methods. But it is not as accurate in the computation of the dipole moment, since the charge density is not really known. However we can make, to some extent, judgements on the agreement of the experimental IR data with calculated results by comparing shifts in the frequencies, and *relative change* of IR intensities compared to C_{60}.

Although the cohesive energy of the cage structures is much lower than that of the peanut and dumbell structures, they require much annealing time to be formed, since their arrangement of bonds is quite different from that of C_{60} from which they are supposed to originate. The dumbell and the peanuts however are a (metastable) local minimum near C_{60} in the phase space, and therefore are more likely to form under experimental conditions where the temperature is not too high. Our study has revealed that because of the very similar features of the experimental and calculated IR peaks: namely the satellites around 1600, 1200, and 600 cm^{-1}, and especially the one developed at 875 cm^{-1}, the dumbell is the most likely candidate for the photopolymerized C_{60} dimers of our experiments. Some of the specific electronic and vibrational features of this structure have also been discussed. This is, to our knowledge, the first quantitative comparison between calculated and experimental IR spectra, and shows, as said previously, that the dumbell structure is indeed the one formed under UV illumination.[10]

ACKNOWLEDGMENTS

The authors would like to express their thanks to the Materials Information Science Group of the Institute for Materials Research, for their continuous support of the HITAC S-3800/380 supercomputing facilities, and to Professor K. Ohno of IMR for useful discussions. K.E.S. acknowledges financial support from an IBM-Hitachi grant.

[1] D. L. Strout, R. L. Murry, C. Xu, W. C. Eckhoff, G. L. Odom, and G. E. Scuseria, Chem. Phys. Lett. **214**, 576 (1993).
[2] G. B. Adams, J. B. Page, O. F. Sankey, and M. O'Keeffe, Phys. Rev. B **50**, 17 471 (1994).
[3] A. M. Rao *et al.*, Science **259**, 955 (1993).
[4] J. Kürti and K. Németh, Chem. Phys. Lett. **256**, 119 (1996).
[5] P. R. Surján and K. Németh, Solid State Commun. **92**, 407 (1994).
[6] D. A. Dixon, B. E. Chase, G. Fitzgerald, and N. Matsuzawa, J. Phys. Chem. **99**, 4486 (1995).
[7] M. R. Pederson and A. A. Quong, Phys. Rev. Lett. **74**, 2319 (1995).
[8] I. O. Bashkin *et al.*, J. Phys. Condens. Matter **6**, 7491 (1994).
[9] A. Kasuya (private communication).
[10] J. Onoe and K. Takeuchi, Phys. Rev. B **54**, 6167 (1996).
[11] C. H. Xu, C. Z. Wang, C. T. Chan, and K. M. Ho, J. Phys. Condens. Matter **4**, 6047 (1992).
[12] A. P. Smith and G. F. Bertsch, Phys. Rev. B **53**, 7002 (1996).
[13] P. Giannozzi and W. Andreoni, Phys. Rev. Lett. **76**, 4915 (1996).
[14] G. F. Bertsch, A. P. Smith, and K. Yabana, Phys. Rev. B **52**, 7876 (1995).
[15] D. Bakowies and W. Thiel, Chem. Phys. **151**, 309 (1991); R. E. Stratton and M. Newton, J. Phys. Chem. **92**, 2141 (1988).
[16] P. Giannozzi and S. Baroni, J. Phys. Chem. **100**, 8537 (1994).
[17] E. Osawa (private communication).
[18] M. Menon, K. R. Subbaswamy, and M. Sawtarie, Phys. Rev. B **49**, 13 966 (1994).